The Structure of a Functional Unit from the Wall of a Gastropod Hemocyanin Offers a Possible Mechanism for Cooperativity[†,‡]

Markus Perbandt,[§] Eckhart W. Guthöhrlein,[§] Wojciech Rypniewski,[§,||] Krassimira Idakieva,[⊥] Stanka Stoeva,[#] Wolfgang Voelter,[#] Nicolay Genov,[⊥] and Christian Betzel*[,§]

Institute of Biochemistry and Molecular Biology I, University Hospital Hamburg-Eppendorf, c/o DESY, Building 22a, Notkestrasse 85, 22603 Hamburg, Germany, Institute of Organic Chemistry, Bulgarian Academy of Sciences, Academy G. Bonchev Strasse, Building 9, Sofia 1113, Bulgaria, Institute of Physiological Chemistry, Department of Physical Biochemistry, University of Tübingen, Hoppe-Seyler-Strasse 4, 72076 Tübingen, Germany, and Institute of Bioorganic Chemistry, Polish Academy of Sciences, Noskowskiego 12/14, 61-704 Poznan, Poland

Received November 21, 2002; Revised Manuscript Received February 25, 2003

ABSTRACT: Structure−function relationships in a molluscan hemocyanin have been investigated by determining the crystal structure of the *Rapana thomasiana* (gastropod) hemocyanin functional unit RtH2*e* in deoxygenated form at 3.38 Å resolution. This is the first X-ray structure of an unit from the wall of the molluscan hemocyanin cylinder. The crystal structure of RtH2*e* demonstrates molecular self-assembly of six identical molecules forming a regular hexameric cylinder. This suggests how the functional units are ordered in the wall of the native molluscan hemocyanins. The molecular arrangement is stabilized by specific protomer-to-protomer interactions, which are probably typical for the functional units building the wall of the cylinders. A molecular mechanism for cooperative dioxygen binding in molluscan hemocyanins is proposed on the basis of the molecular interactions between the protomers. In particular, the deoxygenated RtH2*e* structure reveals a tunnel leading from two opposite sides of the molecule to the active site. The tunnel represents a possible entrance pathway for dioxygen molecules. No such tunnels have been observed in the crystal structure of the oxy-Od*g*, a functional unit from the *Octopus dofleini* (cephalopod) hemocyanin in oxygenated form.

In aerobic organisms the reversible binding of dioxygen and its transport from the environment to the tissues are performed by three types of respiratory proteins: hemoglobins/erythrocruorins, hemerythrins, and hemocyanins (Hcs). The members of the last group of dioxygen carriers are giant multisubunit proteins freely dissolved in the hemolymph of invertebrates of two phyla: Mollusca and Arthropoda. Although similar in function, the two types of Hcs[1] are completely different in structure. Molluscan Hcs form hollow cylindrical aggregates, 350 Å in diameter, with an internal collar complex. In cephalopods the basic unit is a decamer built of 350−370 kDa structural subunits whereas in gastropods two decamers, consisting of 400−420 kDa subunits, are assembled face to face to form didecamers with a molecular mass of about 9 MDa. The structural subunit is organized into seven (cephalopods) or eight (gastropods and some cephalopods) approximately 50 kDa functional units (FUs), each of which contains a single dioxygen binding copper site (*1*). These FUs were termed *abcdefgh*. Recently, the complete primary structures of cephalopod (*Octopus dofleini*) and gastropod (*Haliotis tuberculata*) Hc structural subunits have been published (*2*, *3*). FUs *abcdef* of the *H. tuberculata* Hc subunits are "wall domains" and make up the wall of the Hc cylinder, while FUs *g* and *h* form the collar (*4*). In the *Octopus* Hc decamer the collar is formed by 10 FUs *g* (*5*). The X-ray structure of this FU in oxy form has been determined (*6*). However, the mechanism of dioxygen binding by molluscan Hcs has not been examined in detail so far. Upon reaction with dioxygen, which binds as a peroxide ion, Cu(I) is oxidized to Cu(II), and the colorless deoxygenated protein turns blue. The cooperativity decreases upon dissociation of the aggregates (*1*). It seems that the cooperative unit corresponds in size to the subunit polypeptide chain or, under some circumstances, to its dimer (*7*).

Rapana thomasiana is a prosobranch gastropod originally found at the coast of Japan, in the Yellow Sea and in East China Sea. In the middle of the last century this marine snail was discovered at the west coast of the Black Sea where it adapted. Two physicochemically distinct isoforms of the *Rapana* Hc were isolated and characterized (*8*). In previous publications we have described the arrangement of the FUs within the polypeptide chains of the two isoforms (*9*, *10*) and the complete amino acid sequences of the FUs RtH2*a* (*11*) and RtH2*e* (*12*).

[†] The authors acknowledge financial support from the Internationales Büro des BMBF, Bonn, Germany, Grant BUL-99-001, and the Bulgarian National Foundation for Scientific Research, Grant X-717. N.G. thanks NATO for financial support under Grant LST.EV.978185.

[‡] The coordinates for the structure of the *Rapana* hemocyanin functional unit are deposited at the Protein Data Bank with the PDB code 1LNL.

* To whom correspondence should be addressed. Tel: +49-40-8998-4744. Fax: +49-40-8998-4747. E-mail: Betzel@unisgi1.desy.de.

[§] University Hospital Hamburg-Eppendorf.

[||] Polish Academy of Sciences.

[⊥] Bulgarian Academy of Sciences.

[#] University of Tübingen.

[1] Abbreviations: Hc, hemocyanin; FU, functional unit.

10.1021/bi020672x CCC: $25.00
Published on Web 05/09/2003

More structural information about molluscan Hcs is required because it can help to define a mechanism of cooperative oxygen binding (*13*) and can confirm the presence of an unusual cysteine−histidine thioether bond at one of the histidine ligands of the dicopper site (*14*). The role of this bond is still unknown. Up to now there is only limited knowledge about the mechanism of dioxygen binding by molluscan Hcs, and no X-ray structure of a Hc unit from the wall of the cylinders is available. The structure of the *Rapana* Hc FU RtH2*e*, described here, allows a comparison of (a) molluscan Hc FUs in the deoxygenated and oxygenated state, (b) FUs from the "collar" and the wall of molluscan Hcs, and (c) FUs from respiratory proteins of the phylogenetically distinct gastropods and cephalopods.

MATERIALS AND METHODS

Purification and Crystallization of the Functional Unit RtH2e. *R. thomasiana* snails were collected at the west coast of the Black Sea and stored in seawater before extraction of the hemolymph. The crude material was filtered through gauze and centrifuged for 30 min at 4 °C and 5000*g*. Native hemocyanin was sedimented by ultracentrifugation at 40000 rpm and stored at −20 °C in the presence of 20% (w/v) sucrose until used. The FU RtH2*e* from isoform RtH2 was obtained by limited proteolytic digestion. The conditions for the isolation and crystallization of the unit were described previously (*8*−*10*, *15*).

X-ray Structure Analysis. Diffraction data from flash-frozen crystals were collected on a ADSC CCD detector at the Brookhaven National Synchrotron Light Source (BNL) beam line X9A up to 3.38 Å. The X-ray wavelength was 0.98 Å. The space group was assigned to be $P4_32_12$ with cell dimensions of $a = b = 105.5$ Å and $c = 375.0$ Å and three molecules in the asymmetric unit. The calculated Matthews coefficient (*16*) is 3.1 Å^3/Da, which corresponds to a solvent−volume fraction of approximately 60%. The diffraction data were processed using the programs DENZO and SCALPACK (*17*). The phase problem was solved by molecular replacement techniques using the program AMoRe (*18*) and a search model derived from the 2.3 Å structure of the *O. dofleini* hemocyanin functional unit Od*g* (*6*). A rigid body refinement of the initial solution reduced the *R*-factor from 47.2% to 39.9% for all data up to 3.38 Å. The refinement was performed by molecular dynamics techniques using the program CNS (*19*). At each step $2F_o - F_c$ and $F_o - F_c$ maps were calculated to improve the structure in the density maps using the programs TURBO-FRODO (*20*) and O (*21*). Several cycles of positional refinement with restrained individual *B*-factor refinement and rounds of 3000K simulated annealing allowed the correct tracing of flexible loops where the conformations were found to be different from the initial model. Afterward, a maximum likelihood refinement was achieved by the program REFMAC (*22*). No solvent was included in the model to avoid overfitting the limited data at the relatively modest resolution of 3.38 Å. At the two glycosylation sites the first saccharide residue was introduced in the electron density and refined. The refinement of the final model converged to an *R*-factor of 24.7% and an R_{free} of 28.7% for 30824 reflections in the resolution range of 15.0−3.38 Å.

Table 1: Data Collection and Refinement Statistics[a]

space group	$P4_32_12$
a (Å)	105.5
b (Å)	105.5
c (Å)	375.0
resolution limit (Å)	3.38
no. of observations	792618
unique reflections	33066
completeness (%)	99.8 (99.7)
R_{merge} (%)	10.8 (37.3)
I/σ (all)	13.8 (3.7)
resolution (Å)	15−3.38
no. of reflections used in refinement	30824
$R_{crystal}$ (%)	24.7
no. of reflections used in R_{free}	1653
R_{free} (%)	28.7
no. of atoms	
protein atoms	9904
ions	9
average *B* factor (Å^2)	
main-chain atoms	42.8
side-chain atoms	44.5
root-mean-square deviation	
bonds (Å)	0.040
bond angles (deg)	3.100

[a] The values in parentheses correspond to the highest resolution shell (3.55−3.38 Å).

RESULTS

Quality of the Model. The data collection and refinement statistics are summarized in Table 1. The individual protomer chains have geometries close to ideal values with root-mean-square (rms) deviations of 0.040 Å and 3.1° from standard values for bond lengths and angles, respectively. The quality of the model was further checked by PROCHECK (*23*), which showed 70.7% of the non-Gly and non-Pro residues in the most allowed regions of the Ramachandran plot, 27.0% in additionally allowed regions, and only 2.3% in generously allowed regions. As a measure of the stereochemical quality of the model the overall *G*-factor was calculated to be 0.8. This means all quality values are in the range or even better than expected for a protein structure refined at this resolution. The structure of the protomers is based on well-defined electron density. Electron density was not observed for the first five N-terminal residues, and also no ordered solvent molecules were located in the tunnel leading to the active site.

Overall Structure Description. The *Rapana* Hc FU is globularly shaped and has approximate dimensions of 45 × 50 × 70 Å. The accessible surface area for the individual subunit is approximately 16100 Å^2. The polypeptide chain of RtH2*e* consists of 413 residues and is organized into two structural domains (Figures 1 and 2). Figure 2 shows the amino acid sequence of the unit (A) and the secondary structure elements (B). The N-terminal domain (core domain) is mainly α-helical and extends from residues −8 to 305 (Figure 2), according to the numeration adopted after the alignment of the FUs RtH2*e* and Od*g* (*12*). The core domain consists of 12 α-helices termed α_1, α_2, ..., α_{12}, three 3_{10}-helices, designated as G_1, G_2, and G_3, and eight short β-strands (β_1−β_8) (Figure 2B). The surface area calculated only for the core domain is approximately 12120 Å^2. Four α-helices, α_1, α_3, α_6, and α_7, have 18−24 amino acid residues each, the last helix being the longest one. α_7 passes through the center of the domain, and it is antiparallel to α_6. α_1 is almost perpendicular to the other two helices mentioned before. The two domains of RtH2*e* are connected by the helix

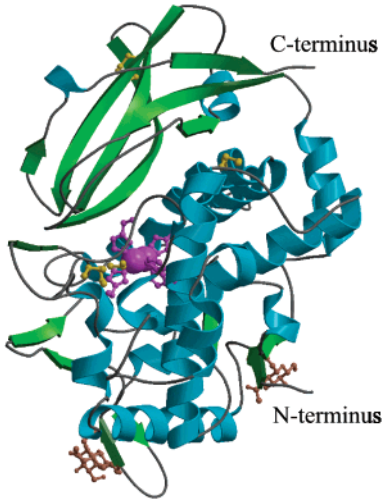

FIGURE 1: Cartoon plot of the *R. thomasiana* hemocyanin functional unit RtH2*e*. The disulfide bridges, active site residues, and carbohydrates are indicated in ball-and-stick representation. Helical regions are shown in blue, β-strands in green, copper atoms and histidine ligands in magenta, and carbohydrates in tan. The three disulfide bonds are shown in yellow. The figure was generated by MOLSCRIPT (*35*).

α_{12}. The N-terminal domain contains two out of the three disulfide bonds found in RtH2*e* and one unusual thioether bridge. The first S−S bond is formed between residues Cys47 and Cys58. Cys171 from helix α_6 and Cys238, located at the beginning of α_8, form the second bridge. On the basis of chemical information (*14*) a covalent bond was introduced and refined with appropriate restraints between S^{γ} of Cys59 and $C^{\epsilon 1}$ of the His61 imidazole, which is one of the copper ligands. Further, there are three proline residues refined in *cis* conformation, Pro44, Pro249, and Pro255. The last one is part of an insertion in comparison to Od*g*. The C-terminal domain is considerably smaller and includes residues 306−405 with a surface area of approximately 5570 Å^2. It contains seven β-strands in β-sandwich topology, labeled β_9−β_{15}, one α-helix, α_{13}, and a short 3_{10}-helix, G_4 (Figures 1 and 2B). There is one disulfide bridge between Cys328, located at the strand β_{10}, and Cys334 from β_{11}. The two domains are connected and stabilized by several hydrogen bonds and one salt bridge between Arg307 and Glu166.

The Molecular Trimer. The asymmetric unit contains three protomers. They interact in a head-to-tail manner and form a noncrystallographic trimer with dimensions of about 45 × 90 × 120 Å. The conformation of the three molecules is nearly identical. Superposition of the three protomers, RtH2e_1, RtH2e_2, and RtH2e_3, showed an rms deviation of 0.9 Å including all Cα atoms, which is affected by the maximum deviation of 11.0 Å caused by differences in the N-terminal region of the protomers. The interface between the first and the second protomer and that between the second and the third are almost identical. A loop (residues 47−60) of the first protomer and nine residues from four different β-sheets (β_{10}, β_{11}, β_{13}, and β_{14}) of the second are involved in protomer-to-protomer interactions (Figure 3). This inter-

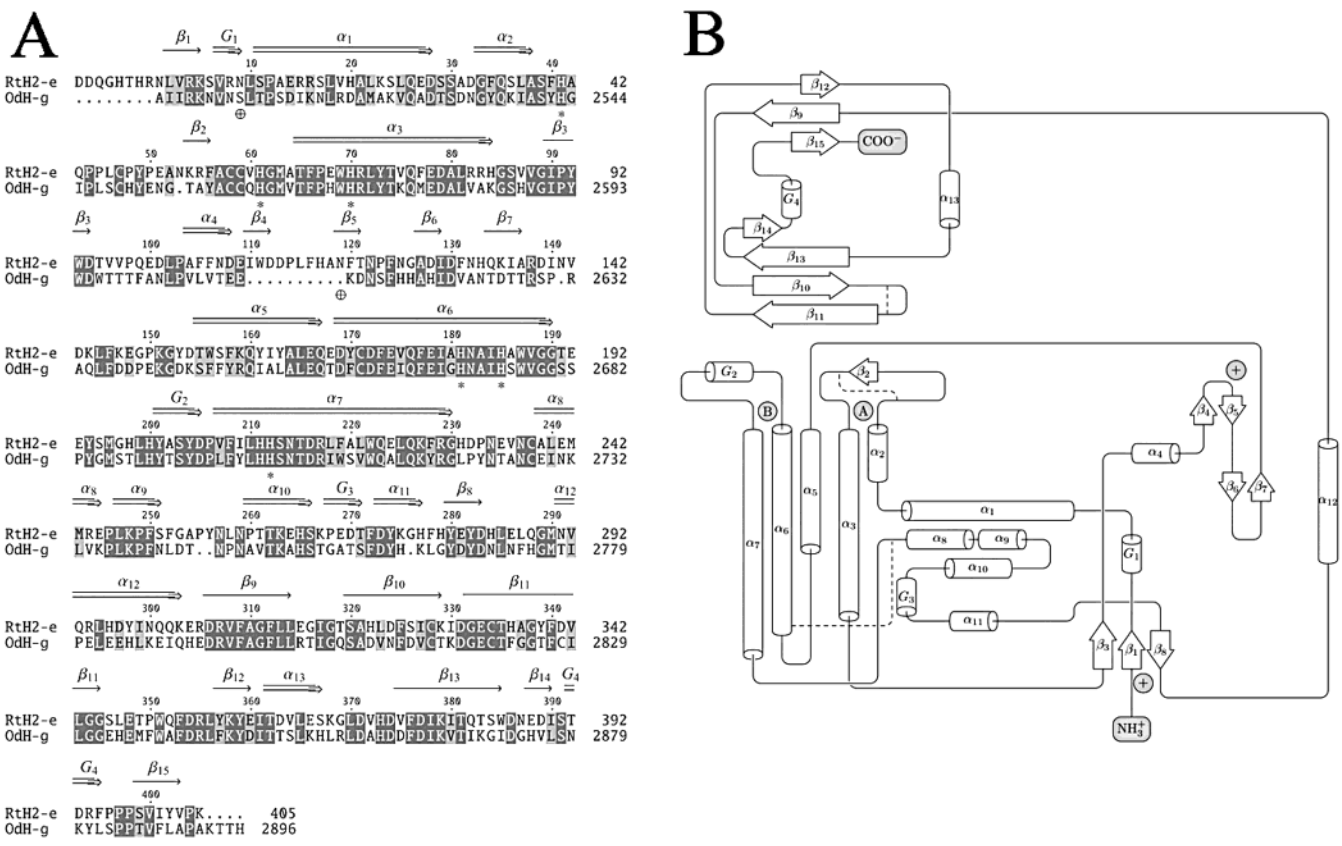

FIGURE 2: (A) Sequence alignment of the *R. thomasiana* and *O. dofleini* hemocyanin functional units RtH2*e* (*11*) and Od*g* (*2*). Identical amino acid residues are shaded in dark gray, and the isofunctional residues are labeled in light gray. α indicates α-helix, β means β-strand, and G is used for the 3_{10}-helix. The histidine ligands for the copper A and B atoms are labeled with an asterisk. The symbol ⊕ indicates the two glycosylation sites at Asn9 and Asn119. The sequence of Od*g* is numbered according to ref *6*, and the sequence of RtH2*e* is numbered according to ref *12*. (B) Secondary structure plot of the *R. thomasiana* hemocyanin functional unit RtH2*e*. α-Helices are indicated as cylinders, β-strands by arrows, disulfide bonds by dashed lines, the two copper ions by A and B, and the two glycosylation sites by ⊕.

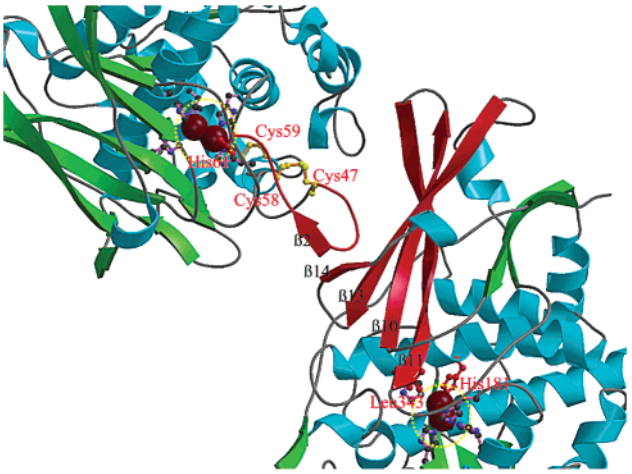

FIGURE 3: Specific protomer-to-protomer interactions in the crystals of the *R. thomasiana* hemocyanin functional unit RtH2*e*. A mechanism for cooperativity of the dioxygen binding is postulated on the basis of the transfer of conformational changes from one active site to the active site region of a neighboring molecule. The directly involved regions and residues are colored in red.

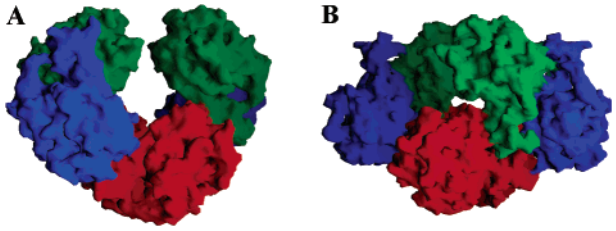

FIGURE 4: Molecular surface of two trimers of the *R. thomasiana* hemocyanin functional unit RtH2*e*, created by the program GRASP (*36*), in two orientations. The protomers are shown in different colors. They interact in a head-to-tail manner, and two trimers are related by a crystallographic 2-fold axis resulting in a regular and almost closed hexameric cylinder. View B is rotated horizontally by 90°.

face or contact region is called the "docking region" and includes residues Lys144, Thr191, His322, Asp324, His336, Tyr339, Thr383, Asp387, and Asp389. Furthermore, two individual trimers are related by a crystallographic 2-fold axis. As a result, a regular hollow cylinder is the repeating component of the crystal lattice (Figure 4).

The Active Site. The dioxygen binding site of RtH2*e* is located near to the domain interface. This site contains two copper ions (A and B), each copper being in a slightly distorted trigonal coordination geometry with the $N^{\epsilon 2}$ atoms of three histidine ligands (Figure 5). Copper A is coordinated by the side chains of His41, His61, and His70 and copper B by His181, His185, and His212. The mean Cu−Cu distance for all protomers in the asymmetric unit is 2.8 Å. Three hydrophobic residues are in van der Waals contact, with the histidine ligands forming a hydrophobic core surrounding the copper active site. This core consists of Phe66, Phe208, and Leu343. One of the most striking features of the RtH2*e* model is a deep tunnel, leading directly from the surface to the active site from two opposite sides of the globule, with a length of approximately 13 and 20 Å, respectively (Figure 6A). Considering van der Waals radii, the diameter of the tunnel is about 3 Å. As mentioned before, at 3.38 Å resolution we could not locate electron density for ordered solvent molecules or ions inside the channel.

Metal Binding Site and Glycosylation. Besides the two active site Cu(I) ions, the model of the monomeric RtH2*e*

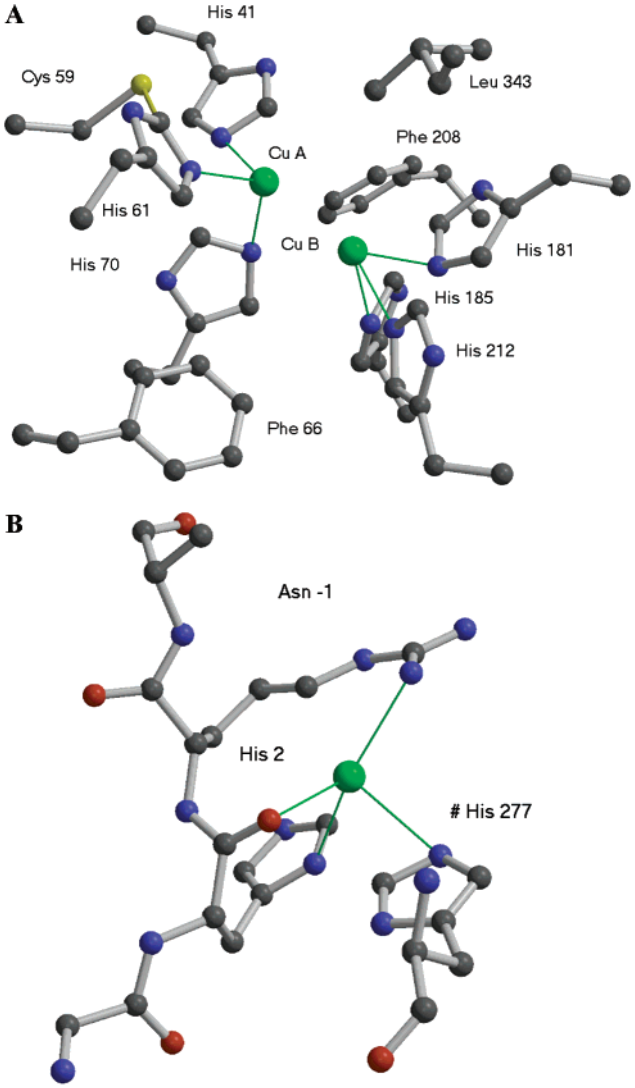

FIGURE 5: (A) Active site residues of RtH2*e* including the thioether bond between Cys59 and His61. The trigonal coordination of the Cu ions is indicated by green lines. (B) This view shows the coordination of the metal ion, which is located at the N-terminus and coordinated by a symmetry-related protomer via His277. The figures were prepared by the programs MOLSCRIPT (*35*) and RASTER3D (*37*).

(Figure 1) contains one additional metal ion, bound at the N-terminal region (Figure 5B). The ligands, coordinating this ion, are $N^{\delta 1}$ of His(−2), NH of Arg(−1), and the carbonyl oxygen of His(−2). The fourth ligand is a histidyl residue of a symmetry-related protomer. At this resolution we could not further identify or characterize the metal ion.

The functional unit RtH2*e* is a glycoprotein with a carbohydrate content of 1.1% (w/w) and monosaccharide constituents xylose, fucose, mannose, and *N*-acetylglucosamine (*12*). Two glycosylation sites at residues Asn9 and Asn119 were identified, showing the first sugar residue of the oligossacharide in the electron density. The first glycosylation site is located at the end of the 3_{10}-helix G_1. The second is part of the short β_5-strand. The two asparagine residues are part of the sequence NXS/T (Figure 2A), typical for asparagine-linked polysaccharides.

DISCUSSION

With the X-ray model described here, the first three-dimensional structure of a deoxygenated form of molluscan

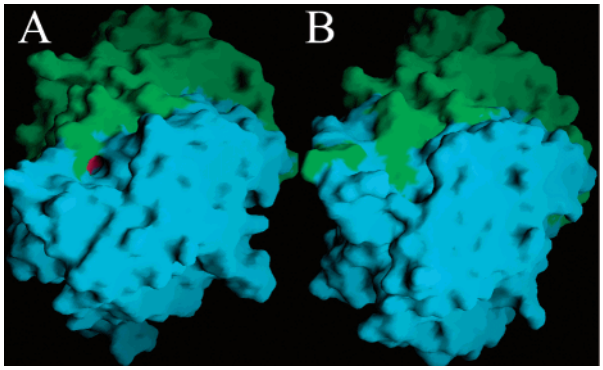

FIGURE 6: (A) Molecular surface of the deoxygenated *R. thomasiana* hemocyanin functional unit RtH2*e*. The N-terminal core domain is colored in blue and the β-sandwich domain in green. A tunnel, leading from the protein surface directly to the active site, is visible. The active site area is shown in red. (B) Identical view of the *O. dofleini* functional unit Od*g* in oxy form. No tunnel (dioxygen entrance pathway) is visible.

Hc FU is now available. A comparison of the deoxy- and oxygenated FUs and a detailed investigation of the interdomain interactions provide structural explanation of some aspects of the molluscan Hc function. The main structural differences between the two FUs can be summarized as follows: (a) the collar unit Od*g* is organized into dimers while six protomers of the "wall-building" RtH2*e* form regular cylinders; (b) in contrast to the functional unit from *O. dofleini*, RtH2*e* contains an N-terminal metal ion binding site. This site connects the protomers of the *Rapana* Hc FU; (c) there is a tunnel from the protein surface of RtH2*e* leading directly to the active site; no such tunnel was found in the structure of Od*g*; (d) there are two glycosylation sites in RtH2*e* in positions different from that of the single carbohydrate binding site in Od*g*; (e) the loop 47−60 has a completely different conformation in deoxy-RtH2*e* and oxy-Od*g*.

The formation of regular cylinders by two symmetry-related trimers is similar to the FU ordering in the wall of native molluscan Hc cylinders. Probably, these interactions are characteristic for the wall-building molluscan Hc FUs. Functional interface residues of the "docking" region, mediating the specific intermolecular contacts between two protomers, are not found in Od*g*. Furthermore, the interface loop region (residues 47−60) has a different conformation in Od*g* with an rms deviation of 5.0 Å in comparison to RtH2*e*. Interestingly, the carbohydrate chain of Od*g* is located at the interface loop 47−60 and imposes in principle a steric hindrance for potential protomer-to-protomer interactions at this site of the molecule. In contrast to RtH2*e*, the FU from the collar of the *O. dofleini* Hc forms dimers, which are similar to the interior collar structure seen in the native molluscan Hcs (*6*, *24*). The three protomers of the *Rapana* Hc FU, located in the asymmetric unit, are linked via an N-terminal metal ion binding site. These interactions contribute also to the stability of the structure and can be essential for the structural organization of the FUs in the wall of the Hc cylinder. No such metal ion binding site has been found in the collar unit *Odg* from the *O. dofleini* Hc.

The amino acid compositions of the two FUs show a predominant negative charge at neutral pH. However, the *R. thomasiana* Hc RtH2*e* is considerably more negatively charged than Od*g* (the net charges are −28 and −14, respectively). This affects the interunit interactions in the Hc aggregates.

The analysis of the interdomain and protomer-to-protomer interactions and conformation offers a potential structural mechanism to explain the modulation of O_2 affinity. It has been shown that the uptake or release of dioxygen affects the active site conformation of the hemocyanin molecule (*25*). The detailed inspection of the RtH2*e* X-ray model revealed a number of significant hydrophobic and hydrogen-bonding interactions between the two domains which are connected by an extensive interface covering a total area of approximately 1630 Å^2. The contact region of the N-terminal domain (core domain) includes helices α_5 and α_6, the following loop, and the region around strand β_2. The C-terminal domain (β-sandwich domain) participates in the interdomain interactions by the surface region immediately after linker helix α_{12}, up to the middle of strand β_9 and the region from the middle part of strand β_{11} until the end of β_{12}. The salt bridge between Arg307 from strand β_9 and Glu166, located at α_5, contributes additionally to the stabilization of the two-domain complex. Leu343 from the β-sandwich domain is in van der Waals contact with His185 of the N-terminal domain active site. This leucine residue is part of a highly conserved LGG motif and is located at the tip of the β-sandwich domain strand β_{11}, which fits well in a concavity of the α-helical domain. Leu343 is conserved in all molluscan hemocyanin sequences determined so far, and it is the only residue of the β-sandwich domain in direct contact to the active site. The copper ligands His181, His185, and His212 are in the immediate proximity of the interface. All three histidyl residues are located in long α-helices. It seems that the active site geometry is very sensitive to changes in the structure and mutual orientation of the two helices. Similar interdomain contacts have been observed in the *Octopus* FU Od*g* (*6*). In summary, the β-sandwich domain can exert some structural effects on the active site located in the core domain. Even slight changes can alter the active site geometry and modulate the dioxygen binding ability.

The RtH2*e* interdomain interactions described above, combined with the interactions between the protomers, offer a mechanism for translation of conformational changes from the active site of one protomer to the active site of the neighboring protomer, as illustrated in Figure 3. The translation of structural changes can induce cooperative effects and could modulate the O_2 affinity. The quaternary structure, formed by the protomers of the *Rapana* Hc FU, is stabilized in the interface region by intermolecular interactions between loop 47−60 of the first protomer and the docking region of the β-sandwich domain of the second protomer. The docking region includes residues from β-sheets β_{10}, β_{11}, β_{13}, and β_{14}. This region is similar to the domain interface and is simultaneously near the active site (Figure 3). Further, loop 47−60 is in the neighborhood of the active site, and its conformation is stabilized by the disulfide bridge Cys47−Cys58. In this context the unusual thioether bridge Cys59−His61 seems to be of great importance. It can play a key role for a cooperative modulation of the O_2 affinity. Upon oxygenation, the Cu−Cu distance and the distances between the copper ions and their ligands will be changed. His61 is one of these ligands, and any structural alteration will be transferred to Cys59 through the covalent bond between S^{γ} of Cys59 and $C^{\epsilon 1}$ of the His61 imidazole. The immediate

neighbor of Cys59 is the disulfide bridge Cys47−Cys58. Any conformational changes in the active site will therefore be conveyed by this disulfide bridge and the thioether bond Cys59−His61. Thus, oxygenation can induce conformational changes in loop 47−60. Accordingly, the conformation of the docking region of the second protomer will be affected, too. In this way conformational changes in the β-sandwich domain can induce changes in the active site geometry of the core domain.

Most probably, the deep tunnel, leading directly from the protein surface to the active site of deoxy-RtH2*e*, forms the entrance pathway for dioxygen molecules from two opposite sides of the molecule. No such tunnel has been observed in oxy-Od*g* (*6*), and a comparison of the two structures demonstrates that the active site of the deoxygenated unit is more accessible than that of the oxygenated one (Figure 6). The active site residues of deoxy-RtH2*e* are clearly visible as shown in Figure 6A (in red). It can be supposed that the binding of dioxygen will induce conformational changes reducing the accessibility to the active site, i.e., that the tunnel is closed after the dioxygen binding. Spectroscopic evidence for conformational changes accompanying oxygenation of arthropod Hcs has already been described (*26*, *27*). The comparison of the two active sites and a superposition of the six histidine residues show that they are homologues. However, the copper−copper distance in deoxy-RtH2*e* is 2.8 Å and is considerably shorter than that of 3.5 Å found in oxy-Od*g* (*6*). This is in contrast to the observation that in the arthropod Hc from *Limulus polyphemus*, upon oxygenation, the copper−copper distance is shortened (*24*). The reason for this difference is not clear. Our results are in agreement with EXAFS studies of deoxy- and oxymolluscan hemocyanin, which demonstrate that upon oxygenation the copper−copper distance slightly increases (*28*, *29*).

The two glycosylation sites in RtH2*e* can be of pharmacological importance, because the high antigenic potency of gastropod Hcs is related to the oligosaccharides bound to their polypeptide chains (*30*). The keyhole limpet Hc (KLH) from *Megthura crenulata* (gastropod), a respiratory protein closely related to the *Rapana* Hc, is widely used in laboratories and clinics as an immune stimulant and in the immunotherapy of bladder cancer and other carcinomas (*31*−*33*). KLH tumor-associated ganglioside conjugates were proposed as possible vaccines in immune therapy of cancer (*34*).

In conclusion, the X-ray structure of the *Rapana* hemocyanin FU RtH2*e* in the deoxygenated state allowed a comparison with the related unit oxy-Od*g*, which revealed important structure−function relationships in the molluscan respiratory proteins. The capability of their subunits to build cylindrical structures is probably due to the specific interactions between the wall-building FUs. This is confirmed by the tendency of the RtH2*e* protomers to form cylinders. The specific intra- and intermolecular interactions in the *Rapana* FU oligomers can be used to propose a cooperative mechanism for translation of information between neighboring active sites based on conformational changes.

ACKNOWLEDGMENT

The authors thank Prof. H. Decker (University of Mainz) and Prof. W. Hendrickson (Columbia University, New York) for providing the coordinates of the functional unit Od*g*.

REFERENCES

1. van Holde, K. E., and Miller, K. I. (1995) *Adv. Protein Chem. 47*, 1−81.
2. Miller, K. I., Cuff, M. E., Lang, W. F., Varga-Weisz, P., Field, K. G., and van Holde, K. E. (1998) *J. Mol. Biol. 278*, 827−842.
3. Lieb, B., Altenhein, B., and Markl, J. (2000) *J. Biol. Chem. 275*, 5675−5681.
4. Meissner, U., Dube, P., Harris, J. R., Stark, H., and Markl, J. (2000) *J. Mol. Biol. 298*, 21−34.
5. Lamy, J., You, V., Taveau, J. C., Boisset, N., and Lamy, J. N. (1998) *J. Mol. Biol. 284*, 1051−1074.
6. Cuff, M. E., Miller, K. I., van Holde, K. E., and Hendrickson, W. A. (1998) *J. Mol. Biol. 278*, 855−870.
7. Klarman, A., Shaklai, N., and Daniel, E. (1975) *Biochemistry 14*, 102−104.
8. Idakieva, K., Severov, S., Svendsen, I., Genov, N., Stoeva, S., Beltramini, M., Tognon, G., Di Muro, P., and Salvato, B. (1993) *Comp. Biochem. Physiol. B 106*, 53−59.
9. Stoeva, S., Dolashka, S., Pervanova, K., Genov, N., and Voelter, W. (1997) *Comp. Biochem. Physiol. B 118*, 927−934.
10. Idakieva, K., Stoeva, S., Pervanova, K., Genov, N., and Voelter, W. (2000) *Biochim. Biophys. Acta 1479*, 175−184.
11. Stoeva, S., Idakieva, K., Genov, N., and, Voelter, W. (1997) *Biochem. Biophys. Res. Commun. 238*, 403−410.
12. Stoeva, S., Idakieva, K., Betzel, C., Genov, N., and Voelter, W. (2002) *Arch. Biochem. Biophys. 399*, 149−158.
13. Kurtz, D. M., Jr. (1999) *Essays Biochem. 34*, 85−100.
14. Gielens, C., De Geest, N., Xin, X. Q., Devreese, B., Van Beeumen, J., and Preaux, G. (1997) *Eur. J. Biochem. 248*, 879−888.
15. Perbandt, M., Chandra, V., Rajashankar, K. R., Idakieva, K., Parvanova, K., Rypniewski, W., Stoeva, S., Voelter, W., Genov, N., and Betzel, C. (2001) *Acta Crystallogr. D 57*, 1663−1665.
16. Matthews, B. W. (1968) *J. Mol. Biol. 33*, 491−497.
17. Otwinowski, Z., and Minor, W. (1996) *Methods Enzymol. 276*, 307−325.
18. Navazza, J. (1994) *Acta Crystallogr. A 50*, 157−163.
19. Brunger, A. T., Adams, P. D., Clore, G. M., DeLano, W. L., Gros, P., Grosse-Kunstleve, R. W., Jiang, J. S., Kuszewski, J., Nilges, M., Pannu, N. S., Read, R. J., Rice, L. M., Simonson, T., and Warren, G. L. (1998) *Acta Crystallogr. 54*, 905−921.
20. Roussel, A., and Cambillau, C. (1991) *Silicon Graphics Geometry Partners Directory*, Silicon Graphics, Mountain View, CA.
21. Jones, T. A., Zou, J. Y., Cowan, S. W., and Kjelgaard, M. (1991) *Acta Crystallogr. A 47*, 110−119.
22. Murshudov, G. N., Vagin, A. A., Lebedev, A., Wilson, K. S., and Dodson, E. J. (1999) *Acta Crystallogr. D 55*, 247−55.
23. Laskowski, R. A., MacArthur, M. W., Moss, D. S., and Thornton, J. M. (1993) *J. Appl. Crystallogr. 26*, 283−291.
24. Lambert, O., Boisset, N., Penczek, P., Lamy, J., Taveau, J. C., Frank, J., and Lamy, J. N. (1994) *J. Mol. Biol. 238*, 75−87.
25. Magnus, K. A., Hazes, B., Ton-That, H., Bonaventura, C., Bonaventura, J., and Hol, W. G. (1994) *Proteins 19*, 302−309.
26. Makino, N. (1987) *Eur. J. Biochem. 163*, 35−41.
27. Leidescher, T., and Decker, H. (1990) *Eur. J. Biochem. 187*, 617−625.
28. Brown, A. R., DeWitt, C. L., Bosma, M. J., and Nisonoff, A. (1980) *J. Immunol. 124*, 250−253.
29. Woolery, G. L., Powers, L., Winkler, M., Solomon, E. I., Lerch, K., and Spiro, T. G. (1984) *Biochim. Biophys. Acta 788*, 155−161.
30. Stoeva, S., Rachev, R., Severov, S., Voelter, W., and Genov, N. (1995) *Comp. Biochem. Physiol. B 110*, 761−765.
31. Lamm, D. L., DeHaven, J. I., Riggs, D. R., and Ebert, R. F. (1993) *J. Urol. 149*, 648−652.
32. Lamm, D. L., DeHaven, J. I., Riggs, D. R., Delgra, C., and Burrell, R. (1993) *Urol. Res. 21*, 33−37.
33. Harris, J. R., and Markl, J. (1999) *Micron 30*, 597−623.
34. Jennemann, R., Gnewuch, C., Bosslet, S., Bauer, B. L., and Wiegandt, H. (1994) *J. Biochem. (Tokyo) 115*, 1047−1052.
35. Kraulis, P. J. (1991) *J. Appl. Crystallogr. 24*, 946−950.
36. Nicolls, A., Sharp, K., and Hornig, B. (1991) *Proteins: Struct., Funct., Genet. 11*, 281−296.
37. Merrit, E. A., and Bacon, D. J. (1997) *Methods Enzymol. 277*, 505−524.

BI020672X